Geochemistry of modern sediments from San Quintín coastal lagoon, Baja California: Implication for provenance

Luis Walter Daesslé[1,2,*], Gabriel Rendón-Márquez[3], Víctor F. Camacho-Ibar[1], Efraín A. Gutiérrez-Galindo[1], Evgueny Shumilin[4], and Eduardo Ortiz-Campos[1]

[1] Universidad Autónoma de Baja California (UABC), Instituto de Investigaciones Oceanológicas , Carretera Tijuana-Ensenada Km. 107, 22830 Ensenada, Baja California, Mexico.
[2] Friedrich Alexander Universität Erlangen-Nürnberg FAU, Institut für Geologie und Mineralogie, Lehrstuhl für Angewandte Geologie, Schloßgarten 5, 91054 Erlangen, Germany.
[3] Centro de Investigación Científica y Educación Superior de Ensenada (CICESE), Departamento de Geología, Carretera Tijuana-Ensenada Km. 107, 22830 Ensenada, Baja California, Mexico.
[4] Instituto Politécnico Nacional-Centro Interdisciplinario de Ciencias Marinas (IPN-CICIMAR), Departamento de Oceanología, Av. IPN. S/N, Col. Playa Palo de Santa Rita, Apdo. Postal 592, 23096 La Paz, Baja California Sur, Mexico.
** walter@uabc.mx*

ABSTRACT

A detailed regional grid of 97 surficial sediment samples is studied for the San Quintín coastal lagoon, which is a shallow embayment located adjacent to a "regionally-rare" intraplate-type basaltic terrain known as San Quintín volcanic field. The influence that this unique lithology and other potential sources have on the recent sediment geochemistry is discussed on the basis of geochemical, petrographic and sedimentological results. The sandy silts and silts in the lagoon are enriched in ferromagnesian minerals such as pyroxenes and hornblende, which form up to 6 and 22%, respectively, of the total mineral count in the sand fraction. These relatively immature feldspathic sediments are characterized by the presence of abundant angular plagioclase (25–60%) and absence of lithics. The La-Sc-Th and Cr-Sc-Th discrimination diagrams suggest that mafic ferromagnesian minerals have a significant effect on the geochemical variance of the sediments. The Cr/Th (median=28) and Co/Th (median=59) ratios are similar to those reported for sands derived from basic rocks. A mafic provenance is probably responsible for the statistical association of Fe, Hf, U, Th, Sc, Cr, Ca, Na and the rare earth elements. An association of Fe, organic carbon and total P with the trace elements Sb, Cr, Br, As, Na, Sc and Co indicates that their distribution is mainly controlled by the presence of Fe-rich minerals, such as hornblende, and organic matter throughout Bahía San Quintín and the northernmost Bahía Falsa, beneath aquaculture racks. Low enrichment factors (<1) for Cr, Sb, As and P indicate that anthropogenic contaminant sources derived from agrochemicals are not significant.

Key words: sediment, geochemistry, volcaniclastic, heavy minerals, phosphorus, coastal lagoon, San Quintín, Mexico.

RESUMEN

Se estudia en detalle una malla regional de 97 muestras de sedimento superficial de la laguna costera de San Quintín. Dicha laguna adyace un terreno basáltico de tipo intraplaca con composición regionalmente atípica, denominado Campo Volcánico de San Quintín. Con base en resultados geoquímicos, petrográficos y sedimentológicos se discute la influencia que tiene la litología característica del campo volcánico, así como otras fuentes potenciales, en la composición del sedimento en la laguna. Los limos arenosos de la laguna están enriquecidos en minerales ferromagnesianos como piroxenos y hornblenda, los cuales forman hasta un 6 y 22%, respectivamente, del conteo de minerales en la fracción de arenas.

Estos sedimentos feldespáticos inmaduros se caracterizan por la presencia de abundante plagioclasa angular (25–60%) y la ausencia de líticos. Los diagramas de discriminación de La-Sc-Th y Cr-Sc-Th señalan que los minerales máficos ferromagnesianos tienen un efecto significativo en la variablilidad geoquímica de los sedimentos. Las razones Cr/Th (mediana= 28) y Co/Th (mediana= 59) son similares a aquéllas reportadas para arenas derivadas de rocas básicas. Una proveniencia máfica es probablemente responsable de la asociación entre Fe, Hf, U, Th, Sc, Cr, Ca, Na y los elementos de las Tierras Raras. La asociación entre Fe, carbono orgánico y P total con los elementos traza Sb, Cr, Br, As, Na, Sc y Co, señala que la distribución de estos elementos está controlada dominantemente por la presencia de minerales de Fe, como la horblenda, y por la materia orgánica a lo largo de Bahía San Quintín y el norte de Bahía Falsa, debajo de los sitios de acuacultura. Los bajos factores de enriquecimiento (<1) para Cr, Sb, As y P indican que la contaminación antropogénica por el aporte de agroquímicos no es significativa.

Palabras clave: sedimento, geoquímica, volcaniclástico, metales pesados, laguna costera, San Quintín, México.

INTRODUCTION

The San Quintín coastal lagoon (SQCL) is a shallow embayment located adjacent to a "regionally-rare" intraplate-type basaltic terrain known as San Quintín volcanic field (SQVF). The SQVF is a group of cinder cones that were active from Pleistocene to Holocene, and probably until historic times (Woodford, 1928; Figure 1). These rocks have an uncommon composition compared with the lithology of the Baja California peninsula. They are composed of alkaline intraplate-type basalts and contain upper mantle peridotite and lower crustal granulite xenoliths (Basu and Murthy, 1977; Rogers *et al.*, 1985; Saunders *et al.*, 1987; Luhr *et al.*, 1995). Stable minerals identified in the basalts are olivine, spinel inclusions, plagioclase, clinopyroxene, titanomagnetite and ilmenite (Luhr *et al.*, 1995). Although the volcanic rocks show varying degrees of erosion and form most of the inner shoreline of SQCL, no evidence for significant weathering of the basalts was found by Gorsline and Stewart (1962). These authors observed uniformity in the mineral composition throughout the bay, which, in addition to the absence of rock fragments and coarse material, led them to conclude that the SQVF only contributed relatively small amounts of sediment to the lagoon.

Recent interest on the biogeochemistry of SQCL has motivated research on the role that the sediment may play as a sink and/or a source of dissolved chemicals in the system. Little is known about the regional heterogeneity of sediment composition and its likely relationship with the biogeochemistry of SQCL. Sediments in the SQCL play an important role in the non-conservative fluxes of dissolved inorganic phosphorus (DIP), and therefore in the primary productivity of this system. Bed sediments act as a net source of phosphorus to the water column because of the organic matter re-mineralization (Camacho-Ibar *et al.*, 2003; Ibarra-Obando *et al.*, 2004). However, the chemical and mineralogical composition of surficial sediments seems to allow them to act as sinks of DIP through sorption during resuspension (Ortiz-Hernández *et al.*, 2004). The finding of uncommonly high Fe and Ti concentrations in the sediments from the SQCL and their heterogenous regional distribution in the SQCL, as well as the lack of correlation of these metals with the mud (silt+clay) grain size fraction, led Navarro *et al.* (2006) to conclude that lithics and/or heavy minerals from the SQVF may be important hosts of these metals in the sediments. Gutiérrez-Galindo *et al.* (2007) suggested that the spatial distributions of Cr and Ni in 39 samples studied from SQCL in 1992 could also be the result of SQVF influence, but that Cd, Cu and Zn could be influenced by upwelling, because of their association with organic matter. No evidence has yet been found for contamination by anthropogenic sources despite the intensive agriculture in the adjacent San Quintín valley and oyster aquaculture in the lagoon. Even though oyster aquaculture can induce changes in shallow coastal ecosystems, including oxygen depletion, alteration of sedimentary geochemical processes, and increased sedimentation beneath culture racks (see Newell *et al.*, 2002; Forrest and Creese, 2006 and references therein), the effect of oyster aquaculture on sediment geochemistry in the SQCL has not been evaluated. Thus characterizing in detail the composition and sedimentology of surface sediments in the SQCL is important not only from the geochemical point of view, but also from an environmental perspective.

In view of the geochemical heterogeneity of modern sediments in the SQCL and the influence of metal-rich volcaniclastic sources, the aim of the present work is to identify the sediment sources to the SQCL using a much wider range of geochemical (including Ca, Na, Fe, Sc, Cr, Co, Br, Ba, Th, U, and rare earth elements), petrographic and sedimentological variables, and a higher sampling resolution than before. The information on surficial sediments (upper 3 cm) of the SQCL floor is used to assess the influence of erosion and/or weathering of metal-rich particles from the SQVF and other sources on the modern sediment geochemistry. In addition, the presence of potential contaminants (P, As, Cr and Sb) associated with input from agrochemicals is assessed. The information in this work is also intended as an important tool for ongoing biogeochemical and biological research projects in the area.

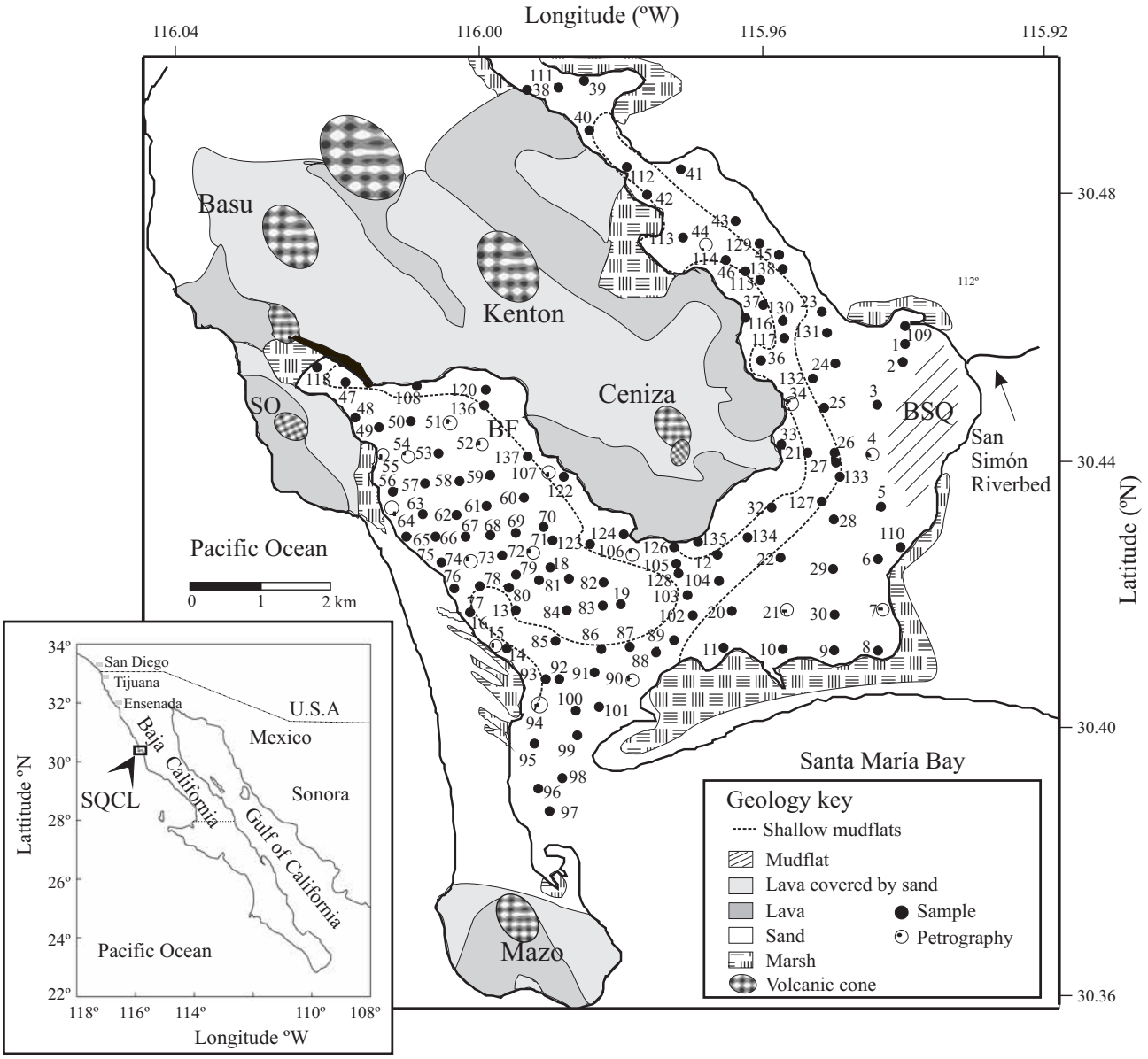

Figure 1. Sampling site location and general geological and geomorphological features in the San Quintín coastal lagoon area (SO: Sudoeste cone; Woodford cone is located to the north, outside the plotted area). Samples analyzed also for petrography are shown in white circles.

REGIONAL SETTING

The SQCL is a shallow coastal lagoon located 350 km south of the Mexico – US Pacific border. Its geomorphology was defined mainly by the eruption of cinder cones belonging to the SQVF and a large dune and beach tombolo separating the lagoon from the Pacific Ocean (Figure 1). The SQCL has an average depth of 2 m, with extensive tidal flats, but with depths that reach 9 m along the tidal channels and the region adjacent to the mouth connecting it with the ocean (Figure 1). It is divided in two sections: Bahía Falsa (BF) and Bahía San Quintín (BSQ). Most of the rocks surrounding the SQCL originated from strombolian volcanic eruptions forming pyroclastic and lava deposits covering an area of 50 – 5000 m^2 (Luhr *et al.*, 1995). The coastal plain is composed of beach sands and fluvial gravel. East of the SQCL (~40 km) crop out the plutons belonging to the Peninsular Range batholith, and andesites and rhyolite tuffs from the Alisitos Formation (Gastil *et al.,* 1975).

The climate in the region is dry with a mean annual rainfall of 150 mm and a mean evaporation of 1400 mm. There is little freshwater and sediment supply from land, as the San Simón watercourse, the main stream draining into the bay, is dry most of the time. Land inputs through this stream seem to occur only during winters of wet years, for example, under El Niño conditions. Tides are mixed

Table 1. Mineralogy of selected sediments from the San Quintín coastal lagoon indicated as % of 300 mineral counts. Abundance of pyroxenes + hornblende ranges 5–26%. See also Figure 1 for sample location.

Sample	**4**	**7**	**15**	**21**	**34**	**44**	**45**	**51**	**52**	**64**	**72**	**74**	**90**	**94**	**106**	**107**
Monocrystaline quartz	22	35	33	22	30	49	40	41	20	42	33	38	20	32	30	28
Polycrystaline quartz	4	8	3	0	3	8	0	0	1	0	1	0	4	0	5	1
Ortoclase	9	2	11	11	8	6	5	1	10	18	7	13	10	11	12	18
Plagioclase	48	35	39	37	38	30	39	48	60	34	44	38	37	45	42	25
Volcanic lithics	0	0	0	0	0	0	0	0	0	2	0	0	0	0	0	0
Sedimentary lithics	0	0	0	0	0	0	0	0	0	0	0	0	0	1	0	0
Metamorphic lithics	0	0	0	0	0	0	4	0	0	0	0	0	0	1	0	9
Biotite	1	0	0	5	0	0	0	0	0	0	0	0	0	0	0	2
Muscovite	0	0	0	0	0	0	0	0	0	0	0	0	0	0	0	1
Horblende	12	16	11	17	18	4	6	9	8	5	10	5	22	5	5	11
Pyroxene	4	3	3	4	1	2	2	2	0	0	3	4	4	4	6	3
Opaques	0	1	1	3	2	0	1	0	0	0	1	1	4	0	0	2
Horblende + pyroxene	16	19	14	21	19	6	8	11	8	5	13	9	26	9	11	14
% Q (quartz)	31	54	42	31	42	61	45	46	23	45	40	43	34	36	39	36
% F (feldspar)	69	46	58	69	58	39	50	54	77	55	60	57	66	62	61	53
% L (lithics)	0	0	0	0	0	0	5	0	0	0	0	0	0	2	0	11

semidiurnal with a range of 2.5 m during spring tides. Maximum tidal current velocities occur in the channels, with values up to 160 cm s^{-1} in the mouth (Flores-Vidal, 2006). Hydrodynamic conditions are different in the two bays, as indicated for example by the difference in water exchange time. During summer, water exchange time is approximately one week in BF and three weeks in BSQ (Camacho-Ibar *et al.*, 2003). One of the main biological features related to sediment transport and accumulation in the bay is the ubiquitous presence of seagrass (*Zostera marina* L. and *Ruppia maritima* L.) in the intertidal and subtidal areas (Ward *et al.,* 2003). San Quintín has ~5,021 inhabitants. The most important economic activity in the SQCL is oyster aquaculture, which by regulation is concentrated in BF, where it covers ~300 ha. On land, agriculture is the most important activity.

METHODS

Sediment samples were collected in 2004 on a regional grid with an in-house designed PVC-polyethylene corer designed to retrieve only the upper ~3 cm of the lagoon floor sediments, in order to study the most recent sediments only. Homogenized sub-samples were used for petrographic, particle size distribution and chemical analyses. For petrography, 16 samples from different sites covering the entire SQCL were selected (Figure 1, Table 1). They were wet-sieved, oven dried and impregnated with epoxic resin. Thin slides were cut and stained to identify quartz, K-feldspar and plagioclase, as well as heavy minerals. Three hundred points were counted using a spacing of ~0.1 mm. Particle size distribution was determined by means of a HORIBA LA910 laser/tungsten analyzer, and the % sand (> 62.5 μm), silt (4–62.5 μm) and clay (< 4 μm) reported (Table 2, Appendix). Prior to geochemical analyses, the sediments were finely ground with an agate pestle and mortar. Major, trace and rare earth elements (REE) in the samples were analyzed by means of instrumental neutron activation analysis (INAA), along with duplicates, a laboratory in-house reference material, as well as USGS MAG-1 marine reference sediment. Only those elements determined with analytical bias and precision better than ±15% are discussed. These elements include seven REE, and Na, Ca, Ba, Sc, Cr, Fe, Co, As, Sb, Th, U, Br and Hf. Organic carbon (C_{org}) was determined after eliminating carbonates with 0.5 M HCl overnight and rinsing with deionized water. The C_{org} analyses were carried out with a LECO CHNS 932 elemental analyzer. Total P was determined, after ignition at 550ºC and leaching with 1M HCl, with a Varian Cary 50 spectrophotometer (Aspila *et al.* 1976).

RESULTS

Sediment distribution

Sediments in the SQCL are mainly composed of green and grayish green sandy silts and clay, with clay size particles exceeding 20% mainly in the heads of BF and BSQ, and a localized spot in southern BSQ (Figures 2a and b). Consistently, muds (silt+clay) are found mainly in shallow waters in the heads of BSQ and BF, as well as in central BSQ, where depths are < 2 m. Sands are dominant near the mouth of the bay toward the ocean along the deeper (<9 m) tidal channels and adjacent to the dune and beach sand bar. Coarse sands are absent. Near the discharge site of the San Simón watercourse, silty sands are dominant and no evidence is seen for preferential coarse sediment deposition associated with stream inflow. This arroyo is

Table 2. Summary statistics of grain size distribution and geochemical data for the San Quintín coastal lagoon, and comparison with the compositions of NASC, UCC, average of the Peninsular Ranges batholith, and average of Kenton volcano (San Quintín volcanic field).

Variable	Mean	Median	Std. dev.	Min	Max	n	NASC[a]	UCC[b]	Batholith[c]	Kenton[d]
Clay (%)	7	5	9	0	66	97				
Silt	39	36	27	0	89	97				
Sand	54	58	32	0	100	97				
C_{org}	0.58	0.45	0.49	0.07	2.11	89				
Fe	3.5	3.5	1.1	1.1	5.9	97	3.96	3.92	3.32	8.00
Ca	2.9	2.8	1.4	0.2	6.2	96	2.36	2.57	3.65	6.68
Na	2.1	2.0	0.5	1.0	3.4	97	0.73	2.37	2.69	2.50
P	0.048	0.048	0.011	0.028	0.070	79	(0.074)	0.065	0.06	0.26
Sc ($\mu g\ g^{-1}$)	17.6	18.5	4.4	6.0	28.0	97	14.9	14	14	24.7
Cr	31.6	32.5	12.5	2.3	61.7	97	124.5	92	47	209
Co	25.0	21.1	17.2	11.8	145.8	97	25.7	17.3		45.4
As	2.0	1.7	1.6	0.2	8.3	97	28.4	4.8		
Br	14.7	10.3	13.9	0.3	76.5	97	0.69	1.6		
Sb	0.25	0.20	0.21	0.04	1.21	97	2.09	0.4		
Ba	265	200	206	22	840	96	636	624	641	408
La	13.8	12.5	9.4	1.3	72.8	97	31.1	31	16	33.3
Ce	27.5	25.3	15.5	4.0	112.7	97	66.7	63	35	68.0
Hf	6.3	3.7	8.0	0.1	42.9	97	6.3	5.3		5.6
Nd	13.4	12.9	6.2	3.5	49.0	97	27.4	27	14	32
Sm	3.6	3.5	1.4	1.0	11.5	97	5.59	4.7		7.65
Tb	0.72	0.69	0.31	0.19	2.00	97	0.85	0.7		
Yb	2.1	1.8	1.6	0.3	9.8	97	3.06	2.0		2.60
Lu	0.36	0.31	0.28	0.04	1.74	97	0.456	0.31		0.372
Th	4.4	3.9	3.4	0.2	21.8	97	12.3	10.5	7.2	3.78
U	1.1	1.0	0.7	0.2	3.7	97	2.66	2.7	0.39	1.68

[a] Gromet *et al.* (1984), [b] Rudnick and Gao (2004), [c] Silver and Chappell (1987), [d] Luhr *et al.* (1995).

flooded only occasionally during extreme rainfall, and its riverbed is currently covered by sand and shrubs. Field observations of the extensive sand deposits along the arroyo, marshland along the coastline and the absence of a defined delta structure (*cf.* Gorsline and Stewart 1962), suggest that any occasional sediment input from this source may have been already mixed by the dominant and continuous coastal hydrodynamics.

Petrography

The minerals counted are shown in Table 1. The modal analysis of the sandy fraction shows a high content of plagioclase and quartz (both >75% of total count), and a low K-feldspar content. Lithic fragments are practically absent, probably because coarse sand is also absent. According to the mineralogic classification of Okada (1971), the sands are classified as feldspathic sediment, with plagiocalse dominant relative to K-felspar, and can be classified as having an uplifted basement source (Figure 3; Dickinson *et al.*, 1983). The high abundance of hornblende, monocrystalline quartz and lesser amounts of K-feldspar suggests the importance of the granitic regional basement. Heavy mineral content in the determined samples is as much as 30% of the total mineral count, and includes hornblende, pyroxene, mica (biotite > muscovite) and opaque minerals (magnetite > titanomagnetite). Hornblende and pyroxene are present as euhedral crystals (Figure 4) without evidence for extensive weathering and/or transport, suggestive of a local source. Thus, two predominant mineral sources can be defined for the SQCL: (1) of local volcanic origin belonging to the SQVF, and (2) from the erosion of the batholitic basement. Scanning electronic microscopy (SEM) confirmed the presence of the minerals identified with the petrographic microscope. Owing to its unstable nature, olivine was seldom identified and only as small crystals. Figure 4 shows a pyroxene crystal from the SQCL with a Si, Al, Ca, Mg and Fe general composition, as identified by SEM. This chemical composition, that corresponds to diopside, is only possible from an ultramafic xenolith source from San Quintín, as described by Basu (1975). No chromite or spinel was identified in the samples.

Sediment geochemistry and statistical factor analyses

The raw geochemical results are given in the Appendix and summarized in Table 2. Of all the elements studied, Cr has a unique regional distribution, in that it is relatively

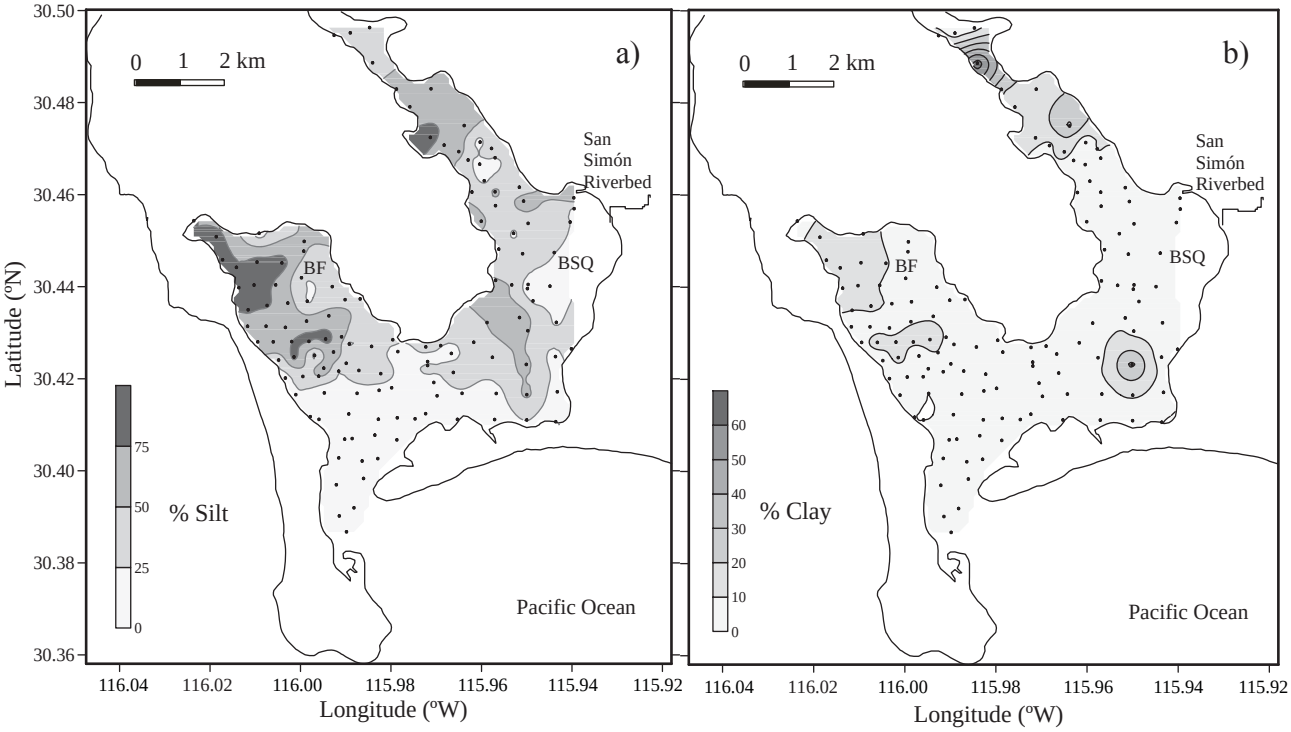

Figure 2. Regional distribution of sediment grain size in the San Quintín coastal lagoon expressed as (a) % silt (4–62.5 μm) and (b) % clay (< 4 μm) sized particles.

enriched adjacent to the entire coast surrounding BF (above average lagoon concentrations), and also in the eastern SQCL, adjacent to the San Simón discharge site (Figure 5). This distribution partially resembles that of Fe, especially near the entrance of the San Simón watercourse (Figure 5b). The regional distribution of P shows enrichment in the head of BF and central BSQ (Figure 5c). Although its distribution is similar to that of Fe, high concentrations are also found in sites where silts are dominant (Figure 2a).

The chondrite normalized REE patterns show a distribution that is similar to that of rocks from the SQVF (Luhr *et al.*, 1995). They are enriched in light REE (LREE) and depleted in heavy REE (HREE) (average La_n/Lu_n ~4). However, some samples show a slight HREE enrichment in relation to the medium REE (MREE). This enrichment is better assessed by using chondrite normalized Tb_n/Lu_n ratios. The Tb_n/Lu_n ratios in the sediments average 1.7 (0.7–4.3), and are similar to those of the SQVF rocks (Luhr *et al.,* 1995), with $Tb_n/Lu_n = 1.9$ (1.7–2.1). The Tb_n/Lu_n ratios in the SQVF and SQCL are only slightly higher than those in the upper continental crust (UCC; Rudnick and Gao, 2004), and in the North American shale composite (NASC; Gromet *et al.*, 1984), which are 1.5 and 1.2, respectively. In order to closer assess any similarities between the REE patterns of the sediments with those of the SQVF, the concentrations of the seven reported REE were normalized to the average REE composition of Kenton volcano (Luhr *et al.*, 1995). Three types of SQVF-normalized REE distributions were empirically identified on the basis of their Tb_n/Lu_n ratios, indicating three different groups in the sediments (Figure 6).

Varimax rotated factor analysis was used to describe the main sediment geochemical components in SQCL and to better explain the sedimentary and/or hydrodynamic factors controlling sediment composition. In addition to

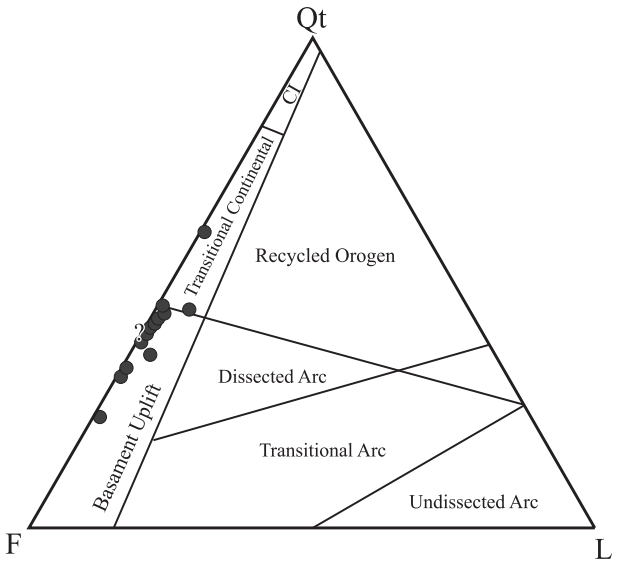

Figure 3. Triangular diagram showing the mineral composition (Qt-F-L) of 17 selected sediments from the San Quintín coastal lagoon (see Table 1) classified as having a dominant uplifted basement provenance. Qt: total monocrystalline and polycrystalline quartz; F: total feldspar; L: total lithic fragments; CI: craton interior (provenance fields after Dickinson *et al.*, 1983).

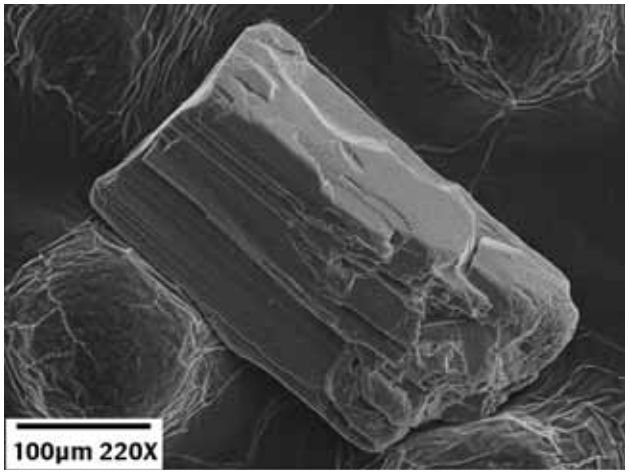

Figure 4. SEM photograph of a euhedral pyroxene crystal commonly found in the SQCL sediments with a general Si-Al-Ca-Mg-Fe composition.

the elements determined with INAA, the factor analysis includes results for abundance of sand, silt, clay, C_{org}, and P. Only those samples for which all the mentioned variables could be determined, were used for statistical analyses (n=77; Table 3). Three factors explain 58% of the total geochemical variance in the lagoon. Factor 1 (accounting for 31% of the total variance) groups Fe, Ca, Cr, Na, Hf, Sc, Th, U and the REE. Positive factor scores (>0.3) for this factor are found in most samples from BSQ (except northern BSQ) and in some from western BF (Figure 7a). The second factor groups those sediments with high silt, clay, C_{org} and P content. Positive Factor 2 scores are found in samples from northern and central BSQ, and northern BF (Figure 7b). The third factor groups Fe, C_{org} and P with As, Br, Ca, Co, Cr, Na and Sc. Unlike the first two factors, Factor 3 scores are positive in most of BSQ and only in a few samples in northernmost BF, where the aquaculture racks are located (Figure 7c).

DISCUSSION

Weathering and provenance

Sediments from the SQCL have a relatively low abundance of C_{org} (0.07–2.1%). The absence of lithics in most of the sediments studied suggests that, if any volcanic rock fragments were present, these were rapidly weathered during more humid past conditions, and weathering products were dispersed out of the basin by the active tidal currents and/or are currently buried. This would explain the low abundance of clay-sized sediments in the SQCL, except for a few samples (Figure 2b). Gorsline and Stewart (1962) reported unusual high abundances of hornblende, exceeding 50% of the total heavy mineral counts in the SQCL sediments. These authors however, did not report the presence of pyroxenes identified in the present work as a dominant (as much as 6%) heavy mineral component (Table 1). Thus, it is possible that clinopyroxenes eroded from the SQVF (more likely from the ultramafic xenoliths), remained in the SQCL and were distributed by tidal currents. The angular appearance of these minerals (as well as that of plagioclase) is suggestive of a nearby source and low degree of weathering (Figure 4). Luhr *et al.* (1995) identified clinopyroxenes in several rock samples from the SQVF. Clinopyroxenes (>5%) are found in mounts Kenton, Basu, Woodford and Mazo, mainly as microphenocrysts. Phenocrysts are present in Mount Mazo (at the end of the dune and beach sand tombolo; Figure 1), but are rare in other cones surrounding the lagoon. One phenocrystic pyroxene from mount Mazo is reported to have exceptionally high SiO_2, Cr_2O_3, NiO, and MgO concentrations, whereas clinopyroxene megacrysts analyzed from the

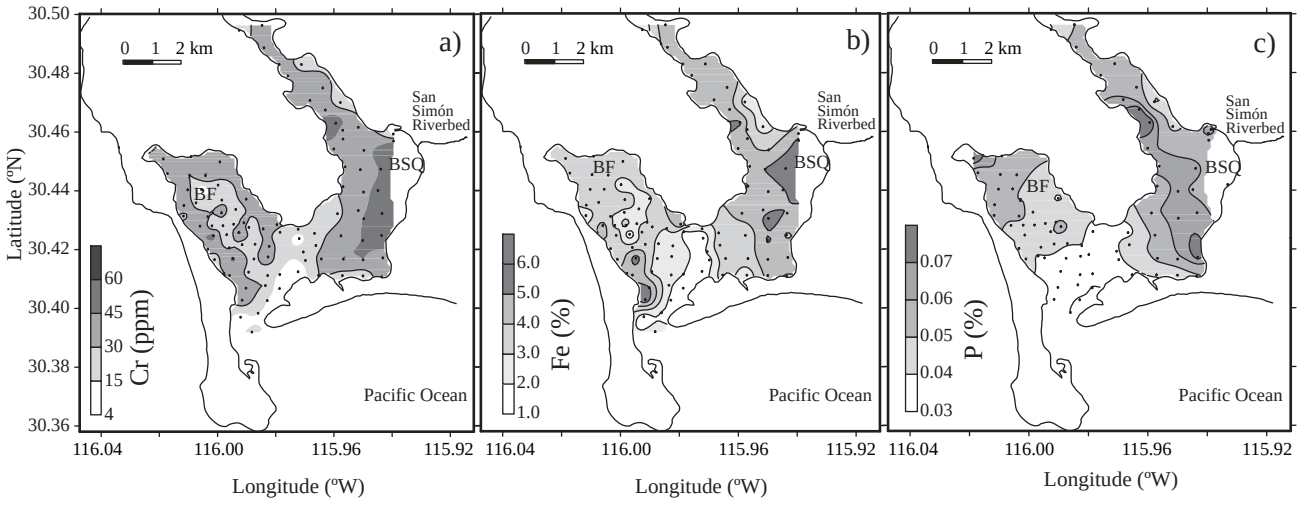

Figure 5. Regional distribution of (a) Cr (µg g^{-1}), (b) Fe (%), and (c) P (%) in modern sediments from the San Quintín coastal lagoon, sampled in 2004.

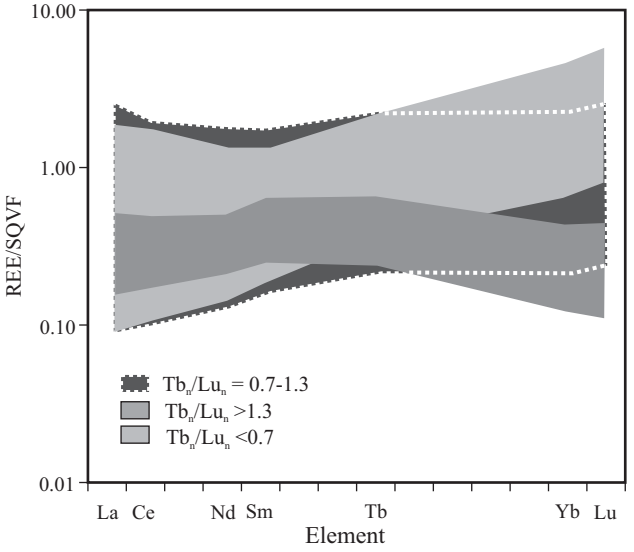

Figure 6. REE patterns of sediments from the SQCL normalized to the average REE concentrations in rocks from Kenton volcano in the SQVF (from Luhr *et al.*, 1995). The normalized distributions are grouped by their Tb_n/Lu_n ratios to indicate MREE/HREE enrichments and depletions.

Woodford complex are characterized by very low Cr_2O_3 and NiO concentrations (<0.02%; Luhr *et al.*, 1995). Oxide mineral microphenocrysts such as Al-Fe-Cr-Mg spinel, spinel inclusions in olivines, groundmass spinel and groundmass ilmenite form >5% of mounts Basu, Kenton and Woodford (Luhr *et al.,* 1995). According to these authors, spinel inclusions may have 24% Cr_2O_3. Chromian spinels are described as being resistant to weathering and abrasion (Pooley, 2004), whereas pyroxenes are only moderately resistant to weathering. Thus, the presence of chromian spinels together with clynopyroxene phenocrysts and microphenocrysts may play an important role in determining the distribution of Fe and Cr in the SQCL (and probably also of V, Co and Ni, as indicated by the partition coefficients of these metals in clinopyroxenes; Rollinson, 1993). However, in the SQCL only a few olivine-bearing, and no spinel-bearing, sediment samples were identified.

Selected element ratios are used to compare the composition of sediments from the SQCL with that published for the SQVF, the Peninsular Ranges batholith, UCC, NASC, post-Archean Australian shale (PAAS) and other sediments eroded from basic and felsic rocks (Table 4; Nagarajan *et al.*, 2007). The La/Sc ratios in sediments from the SQCL (0.1–3.1) are similar to those in the SQVF, and sediments from basaltic rocks. However they are on the lower range of the Peninsular Ranges batholith, UCC, NASC, PAAS and sediment from felsic rocks. This suggests the presence of minerals from a mafic source in sediments in the SQCL, but with an important contribution from felsic rocks (Dokuz and Tanyolu, 2006). High Cr/Th and Co/Cr ratios also suggest a mafic source (Table 4), when compared to the felsic UCC, NASC and PAAS ratios. Sediments with a mafic geochemical signature are ubiquitous in the SQCL, except perhaps those samples adjacent to the dune and beach sand bar (around samples 15, 16 and 94), as well as the inner coast of BF (around sample 107), which also have unusually high REE concentrations (ΣREE >100 μg g^{-1}), and are probably identified as part of the elements associated with heavy minerals in statistical Factor 1. High Cr/Th and Co/Th ratios were also found in the Magdalena–Almejas lagoon (Baja California Sur), adjacent to the Magdalena and Margarita Islands (Table 4), as well as near Cedros Island (Baja California). Enrichments in both areas were probably caused by the weathering and erosion of the ophiolitic rocks in these islands (Daesslé *et al.*, 2000; Rodríguez-Meza, 2005).

Discrimination diagrams (Figures 8 and 9) are further used to assess the geochemical affinity of the sediments with the two most likely geochemical end-members in the region: the SQVF and the Peninsular Ranges batholith, which are located ~40 km east of the SQCL. Although a mixing and integration of the geochemical signatures by the hydrodynamic forces in the lagoon is highly likely, the distinctive composition of the end-members is thought to be reflected to some extent in the sediments. The La-Sc-Th diagram includes the data of the average composition of the Eastern and Western batholith. Sediments from the SQCL have La-Sc-Th compositions that increase in La from a

Table 3. Varimax rotated factor loadings responsible for 58 % of the total variance of sedimentological and geochemical variables in sediments from the San Quintín coastal lagoon (n=77). The highlighted loadings (>0.3) are considered significant (see also Figure 6). The samples used for statistics are highlighted in the Appendix.

Variable	Factor 1	Factor 2	Factor 3
Clay	0.06	**0.76**	0.23
Silt	0.03	**0.93**	0.09
Sand	-0.03	-0.94	-0.13
C	-0.02	**0.47**	**0.65**
Fe	**0.69**	0.05	**0.60**
Ca	**0.65**	-0.35	-0.06
Na	**0.39**	-0.12	**0.66**
P	0.21	**0.40**	**0.76**
Sc	**0.78**	0.04	**0.46**
Cr	**0.55**	-0.14	**0.47**
Co	0.18	-0.04	**0.36**
As	-0.03	-0.35	**0.37**
Br	0.04	**0.33**	**0.75**
Sb	0.17	0.17	**0.49**
Ba	0.04	-0.13	0.25
La	**0.83**	0.05	0.12
Tb	**0.90**	0.15	0.16
Lu	**0.74**	0.16	0.04
Hf	**0.72**	-0.23	-0.38
Th	**0.61**	0.18	0.17
U	**0.46**	0.24	-0.03
% Variance	31	18	9

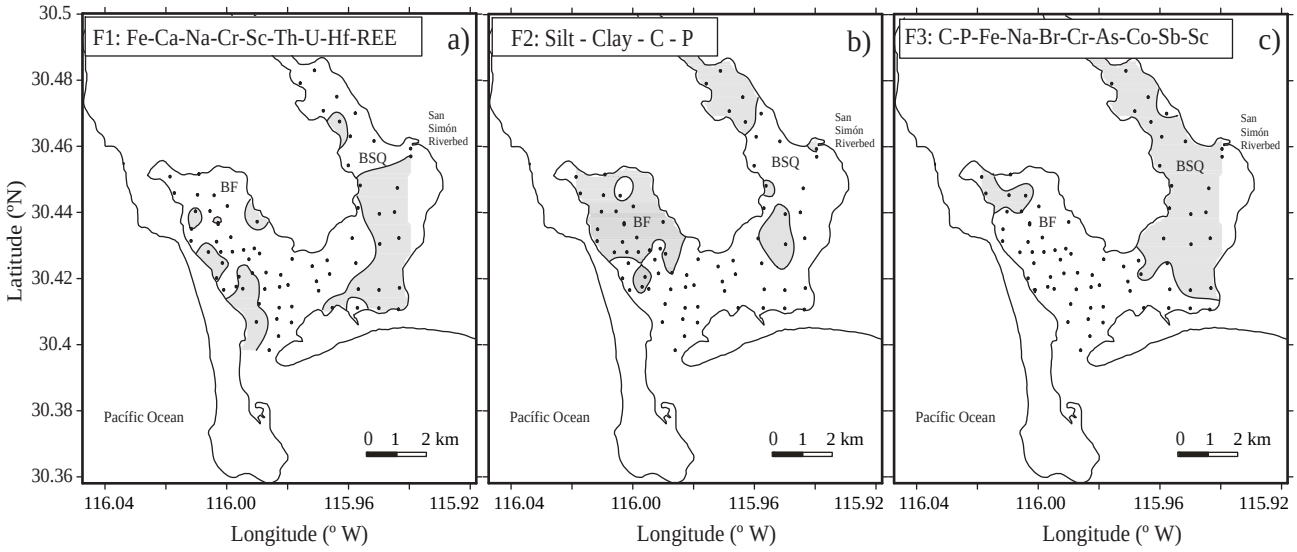

Figure 7. Regional extent of three factor scores, (a) F1, (b) F2 and (c) F3, calculated with varimax rotated factor analysis of grain size and geochemical variables. The 77 samples used for factor analyses are indicated in the Appendix.

batholith-type composition toward and beyond a SQVF composition (Figure 8), suggestive of an additional sediment component enriched in La, probably heavy minerals. Figure 9 shows the proportions of Cr-Sc-Th, in order to assess the potential sources of Cr in the sediment. In the diagram, the sediments show a distribution similar to the trend seen from East to West in the Peninsular batholith rocks (Silver and Chappell, 1987), reaching proportions of Sc comparable to those in the SQVF, but still not the same Th depletion and Cr enrichment as in these rocks. The regional distribution of bulk Cr concentrations strongly suggest that Cr-bearing minerals such as diopside from the xenoliths (with Cr above the average of 30 μg g^{-1}) have preferentially been deposited along the entire coast of BF and throughout BSQ. Mantle-derived ultramafic xenoliths are abundant in the SQVF (Basu, 1975). They are characterized by chromium-diopside rich lherzolite. These rocks are easily friable and may provide the anomalous sources of Sc and Cr in theSQCL. However, a significant enrichment of Cr (along with Fe) along the shallow eastern coast of BSQ (adjacent to the San Simón drainage area), is indicative of peculiar conditions that favor the deposition of these metals there. Since Cr concentrations in the Western batholith (67 μg g^{-1}) are almost three times those from the Eastern batholith (24 μg g^{-1}) (~150 km east), a felsic source for Cr at that specific site (probably as hornblende) could be partially responsible for this enrichment. However, as no opaque minerals (including chromite) were identified in this area, a diagenetic signal may be responsible at least in part for the enrichment in Fe and Cr there, probably as pyrite.

While most of the samples show a similar REE pattern, which is almost identical to that of SQVF rocks, the slight differences in Tb_n/Lu_n (normalized to REE concentrations in SQVF rocks) allow for the identification of two additional factors controlling their distribution (Figure 6). Slight enrichments of HREE along most of the western coast of BF, the southern coast of BSQ and some sites adjacent to the inner coast of BSQ, may indicate the presence (although in small amounts) of minerals such as orthopyroxenes, olivine or other (most likely mafic) minerals enriched in HREE

Table 4. Comparison of elemental ratios of sediments from the San Quintín coastal lagoon (SQCL) and Kenton volcano (San Quintín volcanic field), and comparison with the composition of the Peninsular Ranges batholith, sands from basic (SBR) and felsic rocks (SFR), upper continental crust (UCC), North American shale composite (NASC), post-Archean Australian shale (PAAS), and sediments from Bahía Magdalena (BM) in Baja California Sur.

Elemental	**SQCL**		**Kenton[a]**		**Batholith[b]**	**SBR[c]**	**SFR[c]**	**UCC[d]**	**NASC[e]**	**PAAS[f]**	**BM[g]**
Ratio	Range	Median	Range	Median	Average	Range	Range	Average	Average	Average	Average
La/Sc	0.1–3.1	0.7	0.5–2.5	1.4	1.1	0.4–1.1	2.5–16	2.2	2.1	2.40	1.0
Sc/Th	1.0–90	4.5	0.1–20.8	5.4	1.9	20–25	0.05–1.2	1.3	1.2	1.10	6.0
Cr/Th	1.4–239	28.4	0.9–346	66.0	6.5	22–100	0.5–7.7	8.8	10.1	7.53	178
Co/Th	0.9–186	5.9	10.9–14.2	11.8	-	7.1–8.3	0.22–1.5	1.6	2.09	1.57	17

[a] Luhr *et al.* (1995); [b] Silver and Chappell (1987); [c] Cullers *et al.* (1988) and Cullers (1994); [d] Rudnick and Gao (2004); [e] Gromet *et al.* (1984); [f] Taylor and McLennan (1985); [g] Rodríguez-Meza (2005).

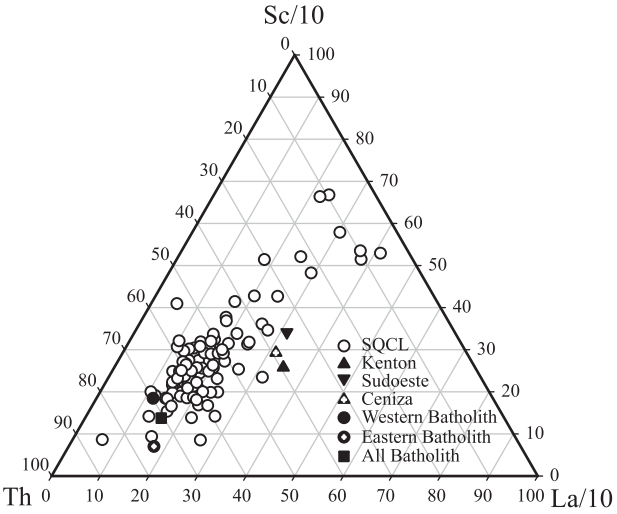

Figure 8. Discrimination diagram of La-Sc-Th for sediments from the San Quintín coastal lagoon (SQCL). Igneous end-members such as the Peninsular batholith and volcanoes from the San Quintín volcanic field are shown for comparison (Silver and Chappell, 1987; Luhr *et al.*, 1995).

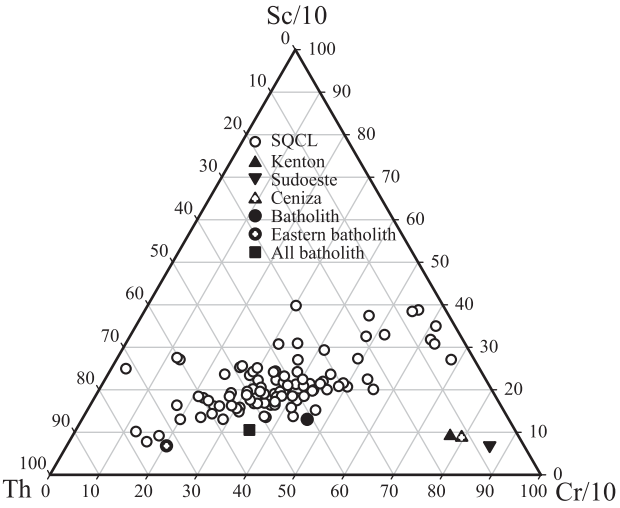

Figure 9. Discrimination diagram of Cr-Sc-Th for sediments from the San Quintín coastal lagoon (SQCL). Igneous end-members such as the Peninsular batholith and volcanoes from the San Quintín volcanic field are shown for comparison (Silver and Chappell, 1987; Luhr *et al.*, 1995).

(Rollinson, 1993). This distribution of samples with Tb_n/Lu_n <0.7 closely resembles that of the factor scores belonging to statistical Factor 1 (Figure 7a), which associates the REE with elements such as Sc, Cr, Hf, U, Th, Ca, Na and Fe.

Grain size effect and element enrichments

Commonly, fine grained particles are a dominant factor controlling metal distribution in aquatic sediments (Lakhan *et al.*, 2003). This suggests the mechanistic link between the sedimentation of organic matter and clastic fines, either through sorption and/or comparable sedimentation conditions. In the SQCL, the abundance of clay and silt are statistically associated only to C_{org} and P, signaling sites of low hydrodynamic energy in the heads of BF and BSQ, as well as in a shallow mud-bank in central BSQ (Figure 2a and b). However, unlike other marine sediments where small grain size is an important factor controlling metal enrichment (Covelli and Fantolan, 1997 and references therein), in SQLC the grain-size effect plays only a secondary role in explaining the compositional variance of the sediments. This is suggested from the bivariate scatter plot of Fe against silt+clay **(**Figure 10a), where no correlation is seen between these variables. Results by Navarro *et al.* (2006) indicate that neither does Al correlate with grain size in the SQCL. This unusual no-correlation between grain size and metal concentrations may be explained by the abundance of Fe-rich hornblende in the fine sand-size fraction throughout SQCL. Thus, normalization against grain size is not an appropriate tool to determine element enrichments in the SQCL. However, Fe appears to control

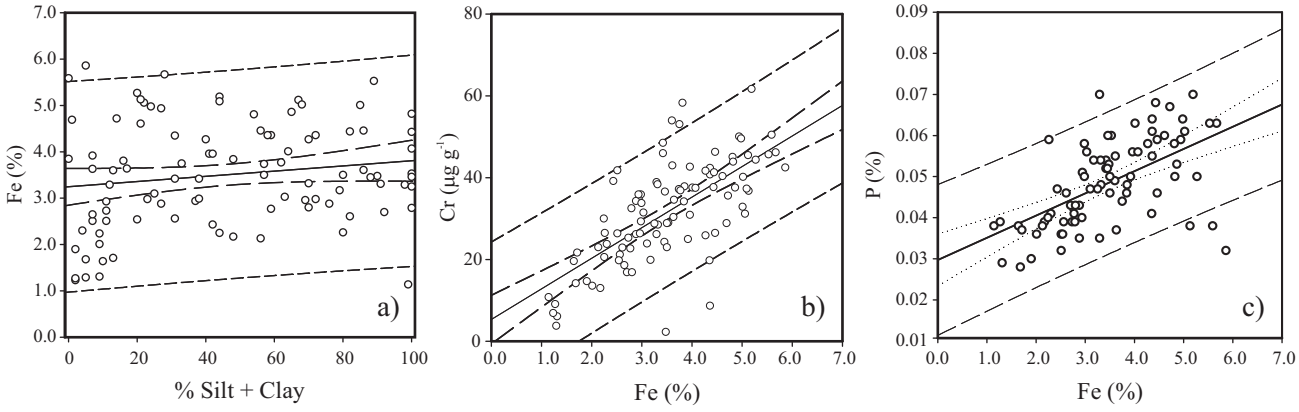

Figure 10. Bivariate scatter plots for (a) silt+clay and Fe with $r^2 = 0.01$, (b) Fe and Cr with $r^2 = 0.47$, and (c) Fe and P with $r^2 = 0.33$ for sediments from the San Quintín coastal lagoon. The dashed lines indicate the confidence interval at 95% and the predicted interval.

part of the enrichment of Cr and P in most of the samples, as suggested by the positive correlation between these elements in the SQCL (Figures 10b and 10c).

The association of Fe in Factor 1, with elements such as Hf, Th, Cr, Sc and the REE indicates that, in parts of BF and BSQ, these elements are contained in heavy minerals (Figure 7a). However, the association of Fe in factor 3 (Figure 7c) with several other trace elements (As, Br, Co, Cr, Sb and Sc), C_{org} and P in BSQ and the northernmost BF (underneath aquaculture sites), may be caused by combined sources in addition to the heavy minerals. Likely additional sediment components that may be responsible for the element association seen in factor 3 are: a) sorption of anions to Fe oxyhydroxides or other Fe minerals; b) formation of authigenic pyrite associated to sediment anoxia in the shallow mud flat adjacent to the mouth of the San Simón watercourse and underneath the aquaculture racks in BF; c) organic matter; and/or d) input of fertilizers containing P, As and Sb (He and Yang, 1999; Otero *et al.*, 2005), or arsenical pesticides (Robinson and Ayuso, 2004) that might be carried from nearby agriculture fields during flooding of the San Simón.

Bromine is an element typically enriched in organic matter formed in saline waters, and shows a strong correlation with organic carbon in sediment (Cosgrove, 1970). This explains the association of Br with C_{org} and P in factor 3. However, considering the relatively low concentration of P, As and Sb (Appendix) in the sediments directly adjacent to the mouth of the San Simón watercourse (samples 1-5 and 109; Figure 1), it is unlikely that these elements were derived from agrochemical pollution. Furthermore, they have low element enrichment factors (EF ≤ 1) when compared to NASC. The EF (calculated as EF = [$element_{sample}/Fe_{sample}$] / [$element_{NASC}/Fe_{NASC}$]) in these samples are 0–0.8 for P, 0.02–0.3 for Cr, 0.01–0.3 for As and 0–0.6 for Sb. Samples throughout SQCL have a mean EF of 0.7, 0.3, 0.1 and 0.1 for P, Cr, As and Sb, respectively. These results indicate that anthropogenic sources for these elements, if any, are minor in the SQCL, and that Fe mineralogy (as heavy minerals and probably diagenetic sulphides) and organic matter are the dominant sediment components controlling the geochemistry of trace elements and P.

CONCLUSIONS

The sediment in the San Quintín coastal lagoon is immature with high feldspar contents relative to quartz and can be classified as having an uplifted basement source. The abundant ferromagnesian minerals have a significant effect on the geochemical variance of SQCL sediments. The presence of ferromagnesian minerals other than hornblende is mainly attributed to their erosion from the San Quintín volcanic field, and their dispersion throughout SQCL by the action of tidal currents, especially near the coastline. Furthermore, elemental ratios (La/Sc, Cr/Th and Co/Th) also suggest a mafic provenance. Discrimination diagrams (La-Sc-Th and Cr-Sc-Th), that include local igneous endmembers and other sediments of known sources for comparison, indicate a dominant felsic source (Peninsular Ranges batholith diorites), with a superimposed mafic (SQVF and its ultramafic xenoliths) secondary heavy mineral source. Factor analyses and REE patterns (especially the normalized MREE/HREE ratios) also suggest a ubiquitous influence of ferromagnesian minerals in the SQCL. No correlation exists between the abundance of mud and the concentration of Fe or other metals, and thus grain size cannot be used as a normalizer for assessing contaminant sources in this coastal lagoon. However, the association of Sb, Cr, Br, As, Na, Sc and Co with Fe, C_{org} and P indicates that, although secondary, the distribution of these trace elements and P is mainly controlled by the presence of Fe-rich minerals such as hornblende (and probably also Fe-oxides and diagenetic Fe-sulphides), and organic matter throughout BSQ and northernmost BF below the aquaculture racks. No evidence for contamination by P, As, Cr and Sb from the use of agrochemicals was found.

ACKNOWLEDGMENTS

We are grateful to V. Guerrero, G. Paniagua and V.A. Macías for their invaluable boating skills while sampling in shallow San Quintín waters. Thanks to E. Navarro for his field and laboratory assistance, A. Siqueiros for helping out with phosphorus analyses, and D. Saposhnikov for INAA analyses. We acknowledge the reviewers of this manuscript for helping us to improve it, especially J. Madhavaraju and A.C. Edwards. Thanks to Prof. H.J Tobschall at the University Erlangen-Nürnberg for his unconditional support and friendship. This work benefited from funding by the Mexican Research and Technology Council CONACYT grant 40144-F to V.F. Camacho-Ibar and a Georg Forster fellowship to L.W. Daesslé from the Alexander von Humboldt Foundation in Germany.

REFERENCES

Aspila, K.I., Agemian, H., Cahu, A.S.Y., 1976, A semi-automated method for the determination of inorganic, organic and total phosphate in sediments: Analyst, 101, 187-197.

Basu, A.R., 1975, Hot-spots, mantle plumes and a model for the origin of ultramafic xenoliths in alkali basalts: Earth and Planetary Science Letters, 28, 261-274.

Basu, A.R., Murthy, V.R., 1977, Olivine-spinel equilibria in lherzolite xenoliths from San Quintín, Baja California: Earth and Planetary Science Letters, 33, 443-450.

Camacho-Ibar, V.F., Carriquiry, J.D., Smith, S.V., 2003, Non-conservative P and N fluxes and net ecosystem production in San Quintin Bay, México: Estuaries, 26, 1220-1237.

Cosgrove, M.E., 1970, Iodine in the Bituminous Kimmeridge shales of the Dorset coast, England: Geochimica et Cosmochimica Acta, 34, 830-836.

Covelli, S., Fantolan, G., 1997, Application of normalization procedure in determining regional geochemical baseline: Environmental

Geology, 30, 34-45.
Cullers, R.L., 1994, The controls on the major and trace element variation on shales, siltstones, and sandstones of Pennsylvanian-Permian age from uplifted continental blocks in Colorado to platform sediment in Kansas, USA: Geochimica et Cosmochimica Acta, 58, 4955-4972.
Cullers, R.L., Basu, A., Suttner, L., 1988, Geochemical signature of provenance in sand size material in soils and stream sediments near the Tobacco root batholith, Montana, USA: Chemical Geology, 70, 335-348.
Daesslé, L.W., Carriquiry, J.D., Navarro, R., Villaescusa-Celaya, J.A., 2000, Geochemistry of surficial sediments from Sebastián Vizcaíno Bay, Baja California: Journal of Coastal Research, 16, 1133-1145.
Dickinson, W.R., Beard, L.S., Brakenridge, G.R., Erjavec, J.L., Ferguson, R.C., Inman, K.F., Knepp, R.A., Lindberg, F.A., Ryberg, P.T., 1983, Provenance of North American Phanerozoic sandstone in relation to tectonic setting: Geological Society of America Bulletin, 94, 222-235.
Dokuz, A., Tanyolu, E., 2006, Geochemical constraints on the provenance, mineral sorting and subaerial weathering of Lower Jurassic and Upper Cretaceous clastic rocks of the Eastern Pontides, Yusufeli (Artvin), NE Turkey: Turkish Journal of Earth Sciences, 15, 181-209.
Flores-Vidal, X., 2006, Circulación residual en Bahía San Quintín, B.C., México: Ensenada, B.C., Mexico, Centro de Investigación Científica y de Educación Superior de Ensenada (CICESE), MSc thesis, 80 p.
Forrest, B.M., Creese, R.G., 2006, Benthic impacts of intertidal oyster culture, with consideration of taxonomic sufficiency: Environmental Monitoring and Assessment, 112, 159–176.
Gastil R.G., Phillips, R.P., Allison, C.C., 1975, Reconnaissance geology of the State of Baja California: Geological Society of America, Memoir 140, 170 p.
Gorsline D.S., Stewart R.A., 1962, Benthic marine exploration of Bahía de San Quintín, Baja California: Pacific Naturalist, 3, 282-319.
Gromet, L.P., Dymek, R.F., Haskin, L.A., Korotev, R.L., 1984, The "North American shale composite": Its compilation, major and trace element characteristics: Geochimica et Cosmochimica Acta, 48, 2469-2482.
Gutiérrez-Galindo. E.A., Muñoz-Barbosa, A., Daesslé, L.W., Segovia-Zavala, J.A., Macias-Zamora, J.V., 2007, Sources and factors influencing the spatial distribution of heavymetals in a coastal lagoon adjacent to the San Quintín volcanic field, Baja California, Mexico: Marine Pollution Bulletin, 54, 1985-1989.
He, M., Yang, J., 1999, Effects of different forms of antimony on rice during the period of germination and growth and antimony concentration in rice tissue: Science of The Total Environment, 243/244,149-155.
Ibarra-Obando, S.E., Smith, S.V., Poumian-Tapia, M., Camacho-Ibar, V.F., Carriquiry, J.D., Montes-Hugo, M., 2004, Benthic metabolism in San Quintin Bay, Baja California, Mexico: Marine Ecology Progress Series, 283, 99-112.
Lakhan, V.C., Cabana, K., LaValle, P.D., 2003, Relationship between grain size and heavy metals in sediments from beaches along the coast of Guyana: Journal of Coastal Research, 19, 600–608.
Luhr, J.F., Aranda-Gómez, J.J., Todd, B.H., 1995, The San Quintin volcanic field, Baja California Norte, México: Geology, petrology, and geochemistry: Journal of Geophysical Reseearch, 100(B7), 10353-10380.
Nagarajan, R., Madhavaraju, J., Nagendra, R., Armstrong-Altrin, J.S., Moutte, J., 2007, Geochemistry of Neoproterozoic shales of the Rabanpalli Formation, Bhima Basin, northern Karnataka, southern India: implications for provenance and paleoredox conditions: Revista Mexicana de Ciencias Geológicas, 24, 150-160.
Navarro, E., Daesslé, L.W., Camacho-Ibar, V.F., Ortíz-Hernández, M.C., Gutiérrez-Galindo, E.A., 2006, The geochemistry of Fe, Ti and Al as an indicator of volcanogenic sedimentation in San Quintín coastal lagoon, Baja California, Mexico: Ciencias Marinas, 32, 205-217.
Newell, R.I.E., Cornwell, J.C., Owens, M.S., 2002, Influence of simulated bivalve biodeposition and microphytobenthos on sediment nitrogen dynamics: a laboratory study; Limnology and. Oceanography, 47, 1367-1379.
Okada, H., 1971, Classification of sandstone: analysis and proposal: Journal of Geology, 79, 509-525.
Ortiz-Hernández, M.C., Camacho-Ibar, V.F., Carriquiry, J.D., Obando, S., Daesslé L.W., 2004, Contribution of sedimentary resuspension to non-conservative fluxes of dissolved inorganic phosphorus in San Quintín Bay, Baja California: An experimental estimate: Ciencias Marinas, 30, 85-89.
Otero, N., Vitòria, L., Soler, A., Canals, A., 2005, Fertiliser characterisation: Major, trace and rare earth elements: Applied Geochemistry, 20, 1473–1488.
Pooley, G.D., 2004, Secondary and backscattered electron imaging of weathered chromian spinel: Scanning, 26, 240–249.
Robinson Jr, G.R., Ayuso, R.A., 2004, Use of spatial statistics and isotopic tracers to measure the influence of arsenical pesticide use on stream sediment chemistry in New England, USA: Applied Geochemistry, 19, 1097–1110.
Rodríguez-Meza, G.D., 2005, Caracterización geoquímica por componentes mayores y elementos traza de sedimentos de los ambientes marinos costeros adyacentes a la península de Baja California Sur: La Paz, Baja California Sur, Mexico, PhD thesis, Instituto Politécnico Nacional, Centro Interdisciplinario de Ciencias Marinas (CICIMAR-IPN), 279 p.
Rogers, G., Saunders, A.D., Terrell, D.J., Verma, S.P., Marriner, G.F., 1985, Geochemistry of Holocene volcanic rocks associated with ridge subduction in Baja California, Mexico: Nature, 315, 389-392.
Rollinson, H., 1993, Using Geochemical Data: Evaluation, Presentation and Interpretation: London, Prentice Hall, 352 p.
Rudnick, R.L., Gao, S., 2004, Composition of the continental crust, *in* Holland, H.D., Turekian, K.K. (eds.), Treatise on Geochemistry, v. 3, The Crust: Amsterdam, Elsevier, 1-64.
Saunders, A.D., Rogers, G., Marriner, G.F., Terrel, D.J. Verma, S.P., 1987, Geochemistry of Cenozoic volcanic rocks, Baja California, Mexico: implications for the petrogenesis of post-subduction magmas: Journal of Volcanology and Geothermal Research, 33, 223-245.
Silver, L.T., Chappell, B.W., 1987, The Peninsular Ranges Batholith: and insight into the evolution of the Cordilleran batholiths of southwestern North America: Transactions of the Royal Society of Edinburgh Earth Science, 79, 105-121.
Taylor, S.R., McLennan, S.M., 1985, The Continental Crust: its Composition and Evolution: Oxford, Blackwell Scientific, 312 p.
Ward, D., Morton, A., Tibbits, T., Douglass, D., Carrera-González, E., 2003, Long-term change in eelgrass distribution at Bahía San Quintín Baja California, México, using satellite imagery: Estuaries, 26, 1529-1539.
Woodford. A.O., 1928, The San Quintín volcanic field, Lower California: American Journal of Science, 15, 337-345.

Manuscript received: June 16, 2008
Corrected manuscript received: Octuber 24, 2008
Manuscript acepted: October 30, 2008

APPENDIX. SAMPLE LOCATION, SEDIMENT DESCRIPTION AND RAW GEOCHEMICAL RESULTS

*Nr.	Lat (ºN)	Long (ºW)	Sediment	% Clay	% Silt	% Sand	C%	P%	Fe%	Ca%	Na%
1	30.4569	115.940	Sand	2	18	80	0.604	0.050	5.27	3.87	2.96
3	30.4474	115.944	Silty sand	3	25	72	0.470	0.063	5.67	5.64	3.17
4	30.4401	115.945	Silty sand	3	24	73	0.575	0.059	4.94	2.93	2.81
5	30.4323	115.943	Silty sand	2	22	75	0.650	0.064	4.98	3.26	3.19
6	30.4248	115.944	Sand	4	12	84	0.296		3.81	3.68	3.43
7	30.4172	115.943	Sand	3	11	86	0.593	0.067	4.72	4.26	3.13
8	30.4107	115.944	Sand	0	0	100	0.171	0.048	3.85	5.38	2.44
9	30.4110	115.950	Silty sand	5	26	69	0.335	0.041	4.35	4.35	2.66
10	30.4947	115.957	Sand	1	3	77	0.117	0.041	2.3	2.82	2.41
11	30.4945	115.965	Sand	1	6	100	0.183	0.037	3.63	4.93	2.44
12	30.4255	115.967	Sand	0	12	88	0.499	0.035	3.29	2.87	2.79
13	30.4169	115.995	Sand	0	0	100	0.142	0.038	5.59	4.88	2.6
15	30.4118	115.998	Sand	0	1	99	0.171		4.69	5.28	1.92
16	30.4166	116.001	Sand	2	23	75	0.423	0.047	3.1	1.76	2.74
19	30.4180	115.980	Sand	5	22	74	0.462	0.035	2.88	4.1	2.56
20	30.4168	115.964	Silty sand	3	14	83	0.381		3.64	4.69	2.64
21	30.4168	115.957	Sand	6	32	62	0.224	0.052	3.42	4.78	2.79
22	30.4247	115.958	Silty sand	7	30	63	0.546	0.051	2.94	4.17	2.55
23	30.4616	115.952	Silty sand	4	38	58	0.497	0.047	2.43	3.29	2.87
24	30.4538	115.950	Silty sand	4	37	59	1.587		3.96	2.71	2.33
25	30.4472	115.951	Silty sand	6	16	78	0.772		5.06	3.83	2.52
27	30.4396	115.950	Sand	7	52	41	0.505	0.061	4.36	1.89	2.6
28	30.4304	115.950	Sandy silt	33	56	10	1.071	0.063	5.53	2.07	2.46
29	30.4231	115.950	Sandy silt	11	56	33	1.227		5.12	2.76	2.55
30	30.4165	115.950	Sandy silt	4	50	46	1.137	0.058	4.81	2.65	2.68
32	30.4322	115.959	Sandy silt	5	51	44	1.640	0.059	4.46	0.8	2.56
33	30.4414	115.957	Sandy silt	9	33	58	1.554	0.056	3.96	4.92	2.5
34	30.4481	115.956	Silty sand	8	56	36	0.912	0.063	4.01	1.83	2.76
36	30.4542	115.960	Sandy silt	2	19	79	1.439	0.060	4.61	2.88	2.49
37	30.4630	115.959	Sand	15	29	56	1.138	0.070	5.19	3.21	2.63
38	30.4946	115.993	Silty sand	5	43	52	0.450	0.039	2.17	2.34	2.29
39	30.4963	115.985	Silty sand	66	34	0	1.245	0.050	4.82		1.94
40	30.4886	115.984	Silty clay	13	59	29	1.096	0.055	4.36	1.93	2.29
41	30.4830	115.971	Sandy silt	14	56	30	0.735	0.058	4.27	3.54	2.49
42	30.4791	115.976	Sandy silt	32	68	0	0.924	0.056	4.07	1.62	2.32
43	30.4750	115.964	Sandy silt	7	58	34	1.228	0.053	4.86	1.07	2.28
44	30.4708	115.968	Sandy silt	12	56	32	1.617	0.061	5.02	1.61	2.31
45	30.4700	115.958	Sandy silt	3	28	69	0.774	0.039	2.56	1.57	2.34
46	30.4675	115.963	Silty sand	14	86	0	1.458	0.068	4.43	2.74	2.29
47	30.4508	116.019	Silt	13	85	2	0.586	0.070	3.29	2.25	2.62
48	30.4459	116.017	Silt	11	75	13	0.756	0.055	3.61	1.32	2.6
50	30.4453	116.010	Silt	11	89	0	1.022	0.060	3.53	2.22	2.71
51	30.4452	116.004	Silt	5	26	70	0.887	0.054	3.42	3.77	2.75
52	30.4419	115.933	Silty sand	10	72	18	0.222	0.046	2.61	2.65	2.37
53	30.4404	116.006	Sandy silt	11	79	10	2.109	0.053	3.48	1.7	2.25
54	30.4403	116.010	Silt	15	85	0	0.881	0.060	3.46	3.1	2.24
56	30.4350	116.012	Silt	10	81	10	1.287	0.054	3.31	2.36	2.32
58	30.4364	116.003	Sandy silt	11	77	12	0.424	0.052	3.45	2.77	2.37
59	30.4368	116.003	Sand	9	61	31	0.262	0.048	3.32	2.66	2.18
60	30.4337	115.927	Sandy silt	9	60	31	0.398		2.96	2.48	2.01
61	30.4325	115.999	Sandy silt	8	68	25	0.200	0.043	2.88	1.51	2.01
62	30.4311	116.003	Sandy silt	7	56	37	0.997	0.056	3.03	1.55	1.75
64	30.4314	116.012	Sandy silt	8	72	20	0.931	0.059	2.26	0.68	1.07
66	30.4280	116.006	Silt-sand-clay	11	75	14	0.279	0.046	4.46	4.51	1.77
67	30.4281	116.002	Silt-sand-clay	12	80	9	0.155	0.043	2.7	3.27	1.8

APPENDIX (cont.)

*Nr.	Lat (ºN)	Long (ºW)	Sediment	% Clay	% Silt	% Sand	C%	P%	Fe%	Ca%	Na%
68	30.4281	115.998	Silt	16	84	0	0.724	0.047	3.25	4.18	1.93
69	30.4286	115.994	Silt	9	61	31	0.281	0.043	2.8	3.61	1.65
70	30.4291	115.991	Sandy silt	3	20	76	0.451	0.050	2.98	3.26	1.53
71	30.4276	115.989	Sand	10	69	21	0.481	0.054	3.17	1.82	1.82
72	30.4258	115.993	Sandy silt	2	11	87	0.383	0.049	3.6	2.43	1.77
73	30.4176	115.997	Sand	13	86	1	0.290	0.038	1.14	0.82	0.95
74	30.4247	116.001	Silt	5	28	67	0.222	0.044	3.75	3.9	1.83
76	30.4201	116.003	Sand	6	42	53	0.104	0.046	3.84	4.72	1.71
78	30.4206	115.996	Sandy silt	9	71	21	0.754	0.050	3.5	3.74	1.7
80	30.4216	115.992	Silty sand	7	50	43	0.135	0.046	3.5	4.8	1.51
81	30.4218	115.987	Sandy silt	9	50	41	0.799	0.041	2.77	2.79	1.66
82	30.4211	115.982	Sandy silt	2	9	89	0.300	0.040	2.93	3.93	1.55
83	30.4175	115.983	Sand	2	9	90	0.068	0.036	2.51	2.82	1.73
84	30.4168	115.988	Sand	1	6	93	0.117	0.032	2.51	2.13	1.8
85	30.4123	115.989	Sand	2	9	89	0.097	0.039	2.73	2.77	1.55
86	30.4112	115.983	Sand	3	17	80	0.107	0.036	2.54	2.1	1.49
87	30.4115	115.979	Sand	2	7	92	0.223	0.036	2.01	0.94	1.74
89	30.4124	115.972	Sand	0	5	95	0.095		1.29	2.28	1.76
90	30.4067	115.979	Sand	1	8	91	0.920	0.029	1.31	0.93	1.36
91	30.4078	115.984	Sand	1	8	91	0.091	0.040	2.24	1.02	1.75
93	30.4069	115.990	Sand	3	18	80	0.104	0.038	5.13	5.59	1.33
94	30.4028	115.992	Sand	1	4	95	0.102	0.032	5.86	6.23	1.6
95	30.3970	115.992	Sand	0	2	98	0.094		1.23	1.22	1.6
98	30.3919	115.988	Sand	1	6	93	0.106		2.65	1.89	1.69
99	30.3983	115.986	Sand	0	2	98	0.083	0.030	1.9	2.88	1.88
101	30.4026	115.983	Sand	0	5	95	0.104	0.028	1.68	2.73	1.81
102	30.4163	115.970	Sand	2	8	90	0.070	0.038	1.64	1.79	1.56
103	30.4192	115.971	Sand	10	46	44	0.191	0.038	2.13	0.44	1.56
104	30.4214	115.966	Sandy silt	1	6	93	0.381	0.050	3.92	1.69	1.47
105	30.4237	115.912	Sand	0	2	98	0.076	0.039	1.27	0.98	1.5
106	30.4259	115.979	Sand	2	11	87	0.078	0.037	1.71	1.03	1.41
107	30.4372	115.990	Silt	11	89	0	0.129	0.039	2.79	2.27	1.6
108	30.4516	116.009	Sand	4	68	28	0.448	0.058	2.98	2.35	1.67
109	30.4593	115.940	Sandy silt	6	52	42	1.990	0.064	4.36	0.31	1.61
112	30.4829	115.979	Clayey silt	22	63	15			5.01	5.44	1.47
117	30.4576	115.957	Silty sand	4	36	60			4.27	3.04	1.62
120	30.4404	115.953	Sandy silt	5	52	43			3.74	4.13	1.86
123	30.4285	115.980	Silty sand	4	34	62			2.99	3.99	1.49
124	30.4269	115.972	Silty sand	4	40	56			5.09	0.19	1.61
126	30.4229	115.972	Silty sand	4	40	57			2.25	2.61	1.42
127	30.4714	115.960	Sandy silt	9	73	18			4.44	3.87	1.28
130	30.4516	115.953	Sandy silt	5	57	38			3.77	2.96	1.48

APPENDIX (cont.)

* Nr.	Ba	Sc	Cr	Co	Se	As	Sb	Th	U	Br	Hf	La	Ce	Nd	Sm	Tb	Yb	Lu
1	65	21.8	44.4	24.8	28.0	1.4	0.3	3.3	1.3	13.7	2.9	14.3	30.8	15.7	4.4	0.8	2.1	0.4
3	365	24.8	46.2	27.2	6.5	3.7	0.2	5.1	1.8	10.0	3.5	14.9	31.8	16.7	4.6	0.8	1.8	0.3
4	425	21.6	50.1	20.9	14.0	2.1	0.2	3.6	0.2	11.3	5.8	10.0	22.6	13.1	3.9	0.9	2.8	0.5
5	840	22.1	49.6	145.8	19.1	1.7	0.2	6.3	0.5	15.6	0.5	21.0	40.0	18.2	4.6	0.8	1.8	0.3
6	275	18.7	58.3	16.3	7.3	2.5	0.3	6.0	0.8	9.8	6.0	15.8	33.0	16.6	4.4	0.9	3.1	0.5
7	300	22.7	35.6	22.0	9.1	1.1	0.5	4.4	0.6	17.6	4.4	16.5	33.9	15.9	4.3	0.9	3.4	0.6
8	155	19.2	37.9	29.0	41.8	0.2	0.3	3.3	0.6	9.6	29.8	10.7	24.7	14.8	4.7	1.0	3.3	0.5
9	155	19.2	19.8	16.6	7.2	1.7	0.5	3.7	1.3	9.3	17.9	19.5	38.2	18.3	4.8	0.9	3.0	0.5
10	43	12.5	23.8	19.5	5.2	4.2	0.0	2.9	1.1	3.0	7.3	9.3	21.7	13.0	4.0	0.5	0.5	0.1
11	50	19.3	30.4	16.5	4.1	5.6	0.4	7.0	1.1	4.2	24.9	24.9	46.3	20.9	5.2	1.0	3.3	0.5
12	155	16.0	26.2	17.4	12.1	1.8	0.2	5.7	0.8	9.9	6.6	22.7	41.0	18.0	4.2	0.7	1.7	0.3
13	135	28.0	50.5	26.3	20.8	2.0	0.2	11.7	3.7	6.7	36.2	52.3	95.3	34.3	7.8	1.9	9.8	1.7
15	750	23.6	28.9	17.0	6.5	3.5	0.0	18.0	1.2	10.1	30.4	72.8	112.7	49.0	11.5	2.0	5.1	0.8
16	545	17.0	23.9	24.8	5.0	3.5	0.1	3.6	0.4	13.1	3.1	13.5	27.7	13.2	3.6	0.7	2.2	0.4
19	175	15.5	26.2	18.5	4.3	1.7	0.1	3.0	0.5	9.1	7.6	20.9	39.0	15.6	3.9	0.8	2.8	0.5
20	515	19.8	34.6	25.5	16.8	1.2	0.2	0.2	1.3	14.5	8.3	15.4	30.1	13.0	3.3	0.6	1.8	0.3
21	395	20.1	46.0	17.6	9.7	0.6	0.2	5.6	1.0	10.3	9.4	24.4	45.2	19.7	4.8	0.8	1.9	0.3
22	67	15.0	34.6	22.1	29.4	1.4	0.4	3.4	1.0	9.8	4.9	8.2	17.9	10.0	2.9	0.6	1.4	0.2
23	465	12.8	39.2	16.3	7.2	5.4	0.5	3.2	0.4	11.1	2.6	6.4	15.1	9.2	2.8	0.6	1.9	0.4
24	120	17.9	42.7	27.8	16.2	1.4	0.1	4.2	0.6	36.2	3.3	17.4	32.2	13.3	3.4	0.7	2.4	0.4
25	265	22.2	31.2	29.3	18.2	5.0	0.7	2.2	2.9	18.8	3.5	9.1	20.8	12.2	3.7	0.7	1.8	0.3
27	320	20.8	40.8	41.8	3.9	0.7	1.2	5.9	1.4	33.8	5.5	18.1	37.0	19.8	5.4	1.6	9.0	1.6
28	94	23.1	45.7	47.7	3.7	2.5	0.4	6.9	1.3	19.2	3.5	15.1	31.8	15.5	4.2	0.8	2.1	0.4
29	195	23.4	45.5	29.2	4.2	5.5	0.2	5.1	0.5	36.9	1.9	16.6	33.3	14.9	4.0	0.8	2.0	0.4
30	755	22.1	45.1	21.2	3.5	1.3	0.1	21.8	2.6	20.4	3.8	15.6	32.3	15.3	4.2	0.8	1.8	0.3
32	105	18.7	26.5	31.1	3.5	2.6	0.8	5.2	0.2	76.5	3.2	13.7	27.6	13.2	3.7	0.6	0.8	0.1
33	115	19.2	30.9	27.9	21.2	5.0	0.8	5.1	1.2	29.9	1.1	14.1	29.0	13.2	3.5	0.8	3.0	0.5
34	51	19.4	37.6	21.7	22.1	0.8	0.5	0.4	0.9	30.1	3.4	14.3	30.9	16.0	4.7	1.2	6.0	1.1
36	280	21.3	40.4	20.6	7.0	4.8	0.1	4.7	0.5	30.3	2.0	17.0	32.7	15.4	4.2	0.9	2.8	0.5
37	360	23.6	61.7	45.2	7.0	8.3	1.0	6.4	0.6	29.8	4.6	18.7	36.7	17.3	4.5	0.8	1.8	0.3
38	410	10.6	13.0	13.5	18.1	2.2	0.1	3.5	0.5	21.5	1.7	8.0	16.3	7.4	2.0	0.4	0.9	0.2
39	97	21.7	43.9	26.5	22.6	2.4	0.2	5.3	0.5	19.8	0.6	14.7	30.8	15.0	4.1	0.7	1.7	0.3
40	140	20.3	42.4	24.2	11.4	2.1	0.2	5.8	1.0	33.6	0.5	16.2	32.7	14.1	3.8	0.7	1.7	0.3
41	200	20.9	25.9	28.1	8.2	3.5	0.5	4.3	1.6	28.9	4.8	15.9	32.8	15.3	4.1	0.8	1.8	0.3
42	400	20.2	37.5	18.4	11.4	1.9	0.2	3.7	1.4	25.5	4.2	11.6	25.3	14.0	4.1	0.9	2.4	0.4
43	150	21.0	37.6	21.3	35.9	0.3	0.5	5.6	2.3	22.6	2.1	16.3	33.2	15.0	4.0	0.7	1.2	0.2
44	210	22.4	40.2	28.5	3.5	2.7	0.3	5.5	1.5	35.6	0.7	12.5	25.9	12.9	3.5	0.6	1.5	0.2
45	55	13.3	21.2	19.3	2.3	0.6	0.1	3.0	0.4	17.6	1.5	7.6	16.1	8.1	2.3	0.4	0.7	0.1
46	750	19.4	37.7	25.8	17.5	2.7	0.2	6.6	2.8	30.3	4.7	17.4	33.3	15.1	4.1	1.1	5.4	1.0
47	61	16.0	38.9	22.1	6.2	2.0	0.4	2.3	1.0	27.4	5.2	12.6	25.0	11.6	3.1	0.5	1.0	0.1
48	500	19.6	43.0	21.1	19.2	1.3	0.2	3.6	0.5	26.2	5.4	9.1	20.8	12.1	3.7	0.8	2.5	0.4
50	185	18.7	29.0	19.8	3.8	0.5	0.1	4.5	1.1	31.5	2.4	11.6	24.9	13.3	3.9	0.8	2.0	0.4
51	445	17.6	48.5	33.7	25.5	1.1	0.1	6.4	2.5	46.4	8.9	13.5	27.2	12.2	3.3	0.6	1.8	0.3
52	410	14.6	22.9	20.5	1.9	1.3	0.2	0.7	3.1	14.8	2.8	8.9	18.8	10.5	3.0	0.7	2.6	0.4
53	175	18.8	2.3	20.7	7.9	1.8	0.5	5.4	1.6	29.3	5.7	21.6	40.0	17.5	4.2	0.9	3.2	0.5
54	53	16.6	36.6	19.4	3.2	0.8	0.5	7.4	1.6	33.9	3.5	17.4	33.3	15.3	4.1	0.9	2.8	0.5
56	185	18.3	38.4	21.7	3.3	0.2	0.4	6.7	1.5	21.4	1.1	14.6	29.7	13.5	3.6	0.9	4.1	0.7
58	330	18.0	24.3	21.1	2.4	1.0	0.4	6.1	0.5	23.1	3.7	18.0	35.6	17.7	4.6	0.9	2.6	0.4
59	135	19.2	28.5	22.6	6.1	0.3	0.5	5.7	0.6	10.8	8.2	20.2	41.0	20.9	5.6	1.0	2.0	0.3
60	380	17.0	26.4	19.0	12.3	3.1	0.1	4.4	1.2	1.9	3.1	11.1	23.0	11.9	3.4	0.6	1.5	0.2
61	265	15.5	34.3	16.9	3.7	3.3	0.0	2.9	0.7	1.0	3.4	12.5	24.8	11.4	3.0	0.6	1.8	0.3
62	74	15.6	31.5	17.2	3.3	1.7	0.1	4.6	0.8	11.0	2.9	13.1	25.3	11.3	3.0	0.6	1.6	0.3
64	22	11.5	26.5	13.9	2.5	1.5	0.1	2.4	1.7	1.1	4.6	6.1	13.3	7.3	2.1	0.5	1.8	0.3
66	200	23.4	46.3	60.9	23.4	1.7	0.4	4.3	0.3	1.2	21.0	14.8	31.8	16.3	4.6	1.0	3.6	0.6
67	305	16.8	16.9	14.5	18.2	2.8	0.4	3.7	1.0	2.1	7.2	11.1	22.6	11.4	3.1	0.6	2.0	0.4
68	140	18.2	28.8	27.2	4.9	5.3	0.2	2.8	0.5	10.2	2.8	9.7	20.8	11.1	3.1	0.8	3.3	0.6

APPENDIX (cont.)

* Nr.	Ba	Sc	Cr	Co	Se	As	Sb	Th	U	Br	Hf	La	Ce	Nd	Sm	Tb	Yb	Lu
69	49	16.4	16.9	23.1	17.3	1.9	0.0	3.1	0.7	1.5	0.2	7.2	16.4	9.9	3.0	0.7	2.1	0.4
70	115	15.8	35.9	24.6	10.3	1.1	0.1	2.2	0.7	8.8	5.6	12.3	25.0	11.9	3.2	0.5	0.9	0.1
71	49	18.4	19.9	18.7	6.7	0.6	0.3	7.4	0.4	3.1	9.8	18.1	35.0	18.0	4.4	0.8	1.9	0.3
72	450	19.4	54.0	19.7	8.2	1.7	0.1	2.3	2.3	2.4	10.2	8.8	19.3	11.2	3.3	0.6	1.6	0.3
73	210	6.0	10.8	12.3	3.9	0.6	0.0	1.2	0.8	2.4	2.0	2.5	5.7	3.5	1.0	0.2	0.5	0.1
74	150	19.8	53.1	19.5	0.6	2.5	0.1	7.2	1.4	0.3	5.5	12.1	27.3	15.4	4.7	0.8	1.8	0.3
76	46	23.8	34.2	20.3	6.0	0.6	0.1	0.3	0.8	0.3	7.5	8.4	19.8	12.9	4.0	0.9	2.8	0.5
78	285	18.5	28.9	20.5	22.4	1.3	0.1	3.3	1.4	11.7	12.0	12.5	25.8	13.0	3.7	0.9	3.4	0.6
80	550	18.6	23.0	27.3	26.0	0.2	0.1	0.8	0.3	1.8	9.2	9.0	20.0	11.8	3.5	0.8	2.6	0.4
81	48	16.4	22.7	16.5	15.3	1.5	0.3	2.8	0.6	4.2	8.4	11.7	22.3	10.0	2.7	0.4	0.8	0.1
82	810	17.5	35.9	16.3	12.8	0.3	0.2	4.1	0.9	1.5	12.0	11.4	22.7	11.5	3.2	0.6	1.7	0.3
83	480	16.6	41.8	55.8	8.5	4.9	0.1	0.3	0.2	0.7	3.3	5.5	13.0	7.9	2.5	0.5	1.0	0.2
84	50	14.7	26.4	21.6	10.4	0.9	0.0	1.3	0.4	1.4	4.1	7.0	15.2	8.1	2.4	0.4	0.7	0.1
85	115	18.5	25.3	14.0	1.2	2.4	0.1	2.5	0.3	2.0	6.2	11.6	24.2	12.6	3.5	0.7	2.0	0.4
86	60	14.3	19.8	14.4	2.4	3.7	0.2	2.5	1.0	1.1	5.3	7.0	15.0	7.5	2.1	0.4	1.2	0.2
87	240	13.4	13.6	19.8	5.5	1.6	0.6	1.7	0.6	0.9	4.8	6.4	15.6	10.1	3.2	0.7	1.8	0.3
89	675	8.0	3.8	15.5	3.7	1.5	0.1	1.8	0.5	0.5	0.5	4.3	9.7	5.4	1.5	0.4	1.4	0.2
90	46	8.0	6.1	15.5	11.5	0.6	0.3	0.6	1.0	0.6	0.5	4.7	9.5	4.5	1.2	0.2	0.5	0.1
91	200	12.6	30.0	18.6	7.5	0.2	0.2	1.4	1.5	0.7	1.4	8.8	17.4	8.5	2.3	0.3	0.5	0.1
93	66	23.9	36.8	19.4	16.1	2.8	0.1	12.3	1.4	2.5	42.9	21.8	42.2	20.4	5.3	1.1	3.2	0.5
94		23.9	42.5	21.1	2.1	0.8	0.1	11.1	1.3	5.5	38.2	37.7	71.7	32.4	8.1	1.7	6.2	1.1
95	145	6.1	6.9	11.8	2.9	0.7	0.1	0.7	0.2	4.7	0.1	4.8	9.7	4.4	1.1	0.2	0.7	0.1
98	330	16.3	18.6	14.7	2.2	1.0	0.1	5.4	1.4	6.3	1.7	17.3	33.1	15.3	4.1	0.8	2.0	0.4
99	325	12.2	14.7	18.2	1.3	2.2	0.1	2.3	1.4	4.9	4.7	4.2	10.6	7.4	2.4	0.5	1.3	0.2
101	305	9.6	14.2	16.2	5.1	2.3	0.0	0.6	1.2	7.3	1.9	3.4	7.4	4.5	1.4	0.2	0.5	0.1
102	130	10.2	19.6	17.4	1.1	0.6	0.1	1.3	0.2	1.4	3.5	1.3	4.0	4.4	1.8	0.3	0.6	0.1
103	810	12.8	23.0	20.3	1.3	1.9	0.3	2.1	1.0	1.9	3.7	8.6	17.2	8.2	2.3	0.3	0.4	0.1
104	81	17.6	25.0	23.6	8.8	5.9	0.1	0.3	0.5	24.5	1.7	12.1	24.7	11.4	3.0	0.4	0.5	0.1
105	140	7.7	9.1	17.7	17.3	1.5	0.3	1.4	0.6	3.0	3.7	2.5	5.8	3.7	1.1	0.3	1.6	0.3
106	325	9.3	21.7	14.6	10.6	3.8	0.2	1.4	0.9	1.1	0.2	4.5	10.1	5.7	1.7	0.2	0.3	0.0
107	225	16.9	32.5	103.9	9.6	0.7	0.2	13.5	1.3	0.8	3.6	28.7	50.2	19.8	4.7	0.7	1.3	0.2
108	24	16.1	29.3	18.7	12.2	0.2	0.2	4.6	0.6	10.9	1.1	9.9	21.3	11.1	3.1	0.6	1.8	0.3
109	115	19.8	8.7	48.0	2.2	0.7	0.4	4.3	1.3	31.5	0.5	9.8	20.0	10.0	2.7	0.5	1.3	0.2
112	645	20.1	32.9	28.4	1.1	1.5	0.0	5.4	2.6	33.1	1.5	12.4	25.1	12.0	3.3	0.6	1.6	0.3
117	195	19.2	41.7	29.8	14.9	1.8	0.0	4.3	1.5	27.2	7.0	10.5	22.3	11.5	3.2	0.6	1.8	0.3
120	620	19.2	37.2	26.0	3.3	0.2	0.1	6.7	1.3	43.5	6.0	10.0	22.6	13.1	3.9	0.7	1.6	0.3
123	270	16.3	33.8	15.0	3.9	1.6	0.1	2.6	2.2	13.9	4.9	8.5	18.3	9.7	2.8	0.6	1.5	0.2
124	310	22.1	37.3	23.3	5.6	0.2	0.1	5.4	1.9	7.3	3.6	12.5	25.5	12.8	3.5	0.7	2.0	0.4
126	340	11.6	20.6	29.8	14.2	0.9	0.3	3.9	1.5	4.0	3.2	13.3	27.0	12.0	3.2	0.6	1.5	0.3
127	435	20.2	41.3	23.4	30.2	1.8	0.4	0.4	1.3	12.9	2.4	10.6	22.2	11.0	3.0	0.6	1.3	0.2

* Nr.: Sample number; samples underlined were used for varimax rotated factor analysis; trace element abundances are reported in $\mu g\ g^{-1}$.